

## ARTICLE

Received 00th January 20xx,  
Accepted 00th January 20xx

DOI: 10.1039/x0xx00000x

## Simple magnesium alkoxides: synthesis, molecular structure, and catalytic behaviour in the ring-opening polymerization of lactide and macrolactones and for copolymerization of maleic anhydride and propylene oxide

Duleeka Wannipurage,<sup>a</sup> Sara D'Aniello,<sup>b</sup> Daniela Pappalardo,<sup>c</sup> Lakshani Wathsala Kulathungage,<sup>a</sup> Cassandra L. Ward,<sup>d</sup> Dennis P. Anderson,<sup>d</sup> Stanislav Groysman,<sup>a\*</sup> Mina Mazzeo<sup>b\*</sup>

The synthesis of two chiral bulky alkoxide pro-ligands: 1-adamantyl-tert-butylphenylmethanol HOAd<sup>t</sup>BuPh and 1-adamantylmethylphenylmethanol HOAdMePh, and their coordination chemistry with magnesium(II) is described, and compared with the coordination chemistry of the previously reported achiral bulky alkoxide pro-ligand HO<sup>c</sup>Bu<sub>2</sub>Ph. Treatment of n-butyl-sec-butylmagnesium with two equivalents of the racemic mixture of HOAd<sup>t</sup>BuPh led selectively to the mononuclear bis(alkoxide) complex Mg(OCAd<sup>t</sup>BuPh)<sub>2</sub>(THF)<sub>2</sub>. <sup>1</sup>H NMR spectroscopy and X-ray crystallography suggested selective formation of *C*<sub>2</sub>-symmetric homochiral diastereomer Mg(OC<sup>R</sup>Ad<sup>t</sup>BuPh)<sub>2</sub>(THF)<sub>2</sub>/Mg(OC<sup>S</sup>Ad<sup>t</sup>BuPh)<sub>2</sub>(THF)<sub>2</sub>. In contrast, the less sterically encumbered HOAdMePh led to the formation of dinuclear products indicating only partial alkyl group substitution. The mononuclear Mg(OCAd<sup>t</sup>BuPh)<sub>2</sub>(THF)<sub>2</sub> complex was tested as catalyst in different reactions for the synthesis of polyesters. In the ROP of lactide, Mg(OCAd<sup>t</sup>BuPh)<sub>2</sub>(THF)<sub>2</sub> demonstrated very highly activity, higher than showed by Mg(OC<sup>c</sup>Bu<sub>2</sub>Ph)<sub>2</sub>(THF)<sub>2</sub>, although with moderate control degree. Both Mg(OCAd<sup>t</sup>BuPh)<sub>2</sub>(THF)<sub>2</sub> and Mg(OC<sup>c</sup>Bu<sub>2</sub>Ph)<sub>2</sub>(THF)<sub>2</sub> were found to be very effective in the polymerization of macrolactones such as  $\omega$ -pentadecalactone (PDL),  $\omega$ -6-hexadecenylactone (HDL) also under mild reaction conditions that are generally prohibitive for these substrates. The same catalysts demonstrated efficient ring-opening copolymerization (ROCOP) of propylene oxide (PO) and maleic anhydride (MA) to produce poly(propylene maleate).

### Introduction

Oil derived plastics are involved in almost every aspect of everyday life. However, their very broad utilization, combined with a lack of forward-thinking strategy regarding their end life, have caused serious environmental pollution. An important challenge for the future is to improve the sustainability of plastics by designing new bio-based materials obtained by low environmental impact procedures.<sup>1, 2</sup> In this context, aliphatic polyesters represent the most promising materials. Depending on the structure of the repeating units they show very different

properties. Aliphatic polyesters having long methylene sequences between ester functionalities are highly hydrophobic materials with tensile properties similar to that of linear low-density poly(ethylene) (LLDPE), and may represent a biodegradable alternative to LLDPE.<sup>3, 4, 5</sup>

The useful synthetic routes for their preparation include the polycondensation of fatty acids<sup>6, 7</sup> and the ring-opening polymerization (ROP) of macrolactones promoted by metal-based,<sup>8, 9</sup> organic catalysts,<sup>10, 11</sup> or enzymes.<sup>12-15</sup>

The chain-growth ROP of macrolactones offers the advantage of a good control over macromolecular parameters such as molecular weights and their dispersity, and end-group fidelity.<sup>16, 8, 11, 17</sup> Unfortunately, macrolactones are insufficiently reactive monomers because they typically do not exhibit ring strain. Therefore, they are rarely polymerized using traditional ROP catalysts and drastic reaction conditions are generally required.<sup>18, 19</sup> To date, relatively few metal-based catalysts active in the ROP of macrolides have been reported, most of them are based on early transition metals<sup>20</sup> and main group metals (Zn, Al, Ca, Mg).<sup>8, 21, 22</sup>

<sup>a</sup> Department of Chemistry, Wayne State University, 5101 Cass Ave. Detroit MI 48202. United States.

<sup>b</sup> Department of Chemistry and Biology "A. Zambelli" University of Salerno, Via Giovanni Paolo II, 132, 84084 Fisciano (SA) Italy

<sup>c</sup> Dipartimento di Scienze e Tecnologie, Università del Sannio, via de Sanctis snc, 82100 Benevento, Italy.

<sup>d</sup> Lumigen Instrument Center, Wayne State University, 5101 Cass Avenue, Detroit, Michigan 48202, United States.

<sup>†</sup> Footnotes relating to the title and/or authors should appear here.

Electronic Supplementary Information (ESI) available: [details of any supplementary information available should be included here]. See DOI: 10.1039/x0xx00000x

An alternative method for the synthesis of polyesters is the ring opening copolymerization of epoxides and anhydrides.<sup>23</sup> The combination of two distinct monomers to form the repeating units of a polyester chain allows the facile access to materials with properties and functionalities not easily reachable by the strict ROP of lactones.<sup>24-26</sup> This synthetic methodology is particularly attractive given the large tolerance toward functional groups within the monomers offering great opportunity for the synthesis of functionalized polymers.<sup>27</sup> Recently, block co-polyesters have been achieved by a chemoselective switch catalysis between the ring opening copolymerization of epoxides and anhydrides and the ROP of lactones or macrolactones.<sup>28, 29</sup>

Generally, the most investigated catalysts for ROP of cyclic esters and for ROCOP of epoxides and anhydrides are heteroleptic complexes of non-toxic metals such as magnesium<sup>30-32</sup> and zinc<sup>33-35</sup>, in which the metal center is coordinated to electronically and sterically tailored ancillary ligands and labile ligand/s that often behave as initiating groups. While this strategy offers the benefits of a very efficient control over polymerization behavior (such as tacticity),<sup>36-38</sup> its disadvantages include somewhat less sustainable nature of the catalyst because of the required multistep synthesis of ancillary ligands. In contrast, recent studies have demonstrated that simple metal-alkoxides or metal-amides, which are commonly used as metal precursors in coordination chemistry, may represent a more sustainable route for polyesters synthesis<sup>39-44</sup> and/or their degradation by alcoholysis.<sup>45, 46</sup>

In 2012 Chen and Cui reported a very simple binary catalyst  $Mg^0Bu_2/Ph_2CHOH$  that showed very high activity in the ROP of lactide (LA), in the presence of a large excess amount of alcohol.<sup>47</sup> In this system the choice of alcohol with bulky substituents proved crucial to promote immortal processes. Subsequently, Dove<sup>48</sup> and Nifant'ev<sup>49</sup> described the use of simple metal alkoxides such as magnesium 2,6-di-tert-butyl-4-methylphenoxy ( $Mg(BHT)_2(THF)_2$ ) for the 'immortal' ring-opening polymerization of caprolactone ( $\epsilon$ -CL) and pentadecalactone (PDL).

Our research groups have previously described the synthesis of a simple magnesium alkoxide  $Mg(OC^tBu_2Ph)_2(THF)_2$  and its reactivity in the polymerization of lactides and the ring-opening copolymerization (ROCOP) of cyclic anhydrides with epoxides demonstrating high efficiency and control in the latter process.<sup>40</sup> As the mononuclear complex  $Mg(OC^tBu_2Ph)_2(THF)_2$  exhibited very high reactivity, we became interested in understanding whether a different steric encumbrance of alkoxide ligand may affect the reactivity of the resulting  $Mg(OR)_2$  pre-catalyst in the ROP of lactones and lactide. Following these findings, we extended our investigations to additional monomers. Furthermore, we became interested in exploring whether a chiral alkoxide can lead to (1) a well-defined  $C_2$ -symmetric structure of a pre-catalyst which could (2) lead to a stereoselective polymerization.

Herein we reported the synthesis of two new chiral bulky alkoxide ligands related to  $[OC^tBu_2Ph]$ ,  $[OC^tBuAdPh]$  and  $[OC^tBuMePh]$ . We demonstrated that while racemic  $[OC^tBuAdPh]$  enables clean formation of homochiral  $C_2$ -

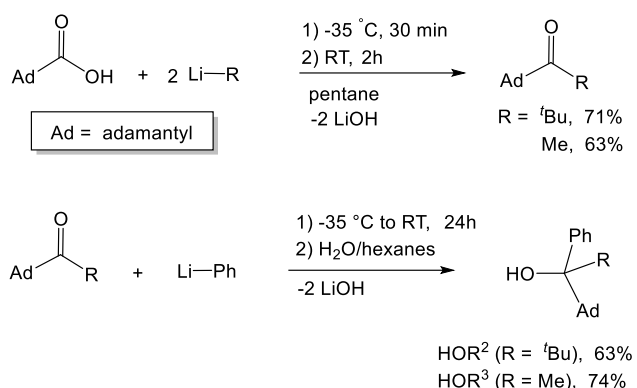
symmetric complex  $Mg(OC^tBuAdPh)_2(THF)_2$ ,  $[OC^tBuMePh]$  did not exhibit well-defined coordination chemistry. The new complex  $Mg(OC^tBuAdPh)_2(THF)_2$ , along with the previously reported  $Mg(OC^tBu_2Ph)_2(THF)_2$ , was investigated as catalyst in the polymerization of lactide, caprolactone and of two macrolactones such as  $\omega$ -pentadecalactone (PDL), and  $\omega$ -6-hexadecenolactone (HDL). Both complexes, in combination with a primary alcohol, were also tested as catalysts for the copolymerization of maleic anhydride and propylene oxide to produce poly(propylene maleate). This polymer can be easily isomerized into poly(propylene fumarate), a 3D printable material to produce thin films and scaffolds that can be modified with bioactive groups by post-polymerization and post-printing functionalization for biomedical applications.<sup>27</sup>

## Results and Discussion

### Design and synthesis of chiral alkoxide ligands $[OC^tBuAdPh]$ and $[OC^tBuMePh]$

We have previously reported the synthesis of  $[OC^tBu_2Ph]$  via the reaction of PhLi with hexamethylacetone and the subsequent synthesis of its transition metal and magnesium complexes, all exhibiting the same mononuclear  $M(OC^tBu_2Ph)_2(THF)_2$  structure.<sup>50-52</sup> In an attempt to investigate formation and coordination chemistry of asymmetric alkoxide ligands, we targeted two bulky asymmetric alkoxide ligands  $[OCAd^tBuPh]$  and  $[OCAdMePh]$ . Both ligands feature very bulky 1-adamantyl substituent and a planar phenyl group; the ligands differ by the third substituent: a relatively large tert-butyl group vs. smaller methyl. Given the (effectively)  $C_{2v}$ -symmetric structures of  $M(OC^tBu_2Ph)_2(THF)_2$  complexes, it is anticipated that the chiral ligands would form diastereomerically pure  $C_2$ -symmetric complexes  $M(OC^R_1R_2R_3)_2(THF)_2$  and  $M(OC^S_1R_2R_3)_2(THF)_2$ . Based on the quadrant model of the transmission of asymmetry, the resulting diastereomerically pure racemic  $C_2$ -symmetric complexes should be capable of stereoselective polymerization if the catalysis takes place in the THF positions, and no exchange of the alkoxide ligands between different enantiomers occurs.

The pro-ligands were synthesized via the intermediacy of the corresponding ketones (1-adamantyl tert-butyl ketone and 1-adamantyl methyl ketone), which can be obtained by the reaction of 1-adamantyl carboxylic acid with the corresponding lithium reagent (Scheme 1). The synthesis of the intermediate ketones and  $HOR^2$  are a modification of the previously reported procedures.<sup>53</sup> Treatment of the ketones with phenyl lithium formed racemic  $HOCAd^tBuPh$  ( $HOR^2$ ) and  $HOCAd^tBuPh$  ( $HOR^3$ ) in 63% and 74% yields, respectively. We note that a different synthetic strategy toward  $HOR^3$  (via the treatment of methyl phenyl ketone via in-situ obtained adamantyl lithium) was recently reported, using a flow microreactor system.<sup>54</sup>

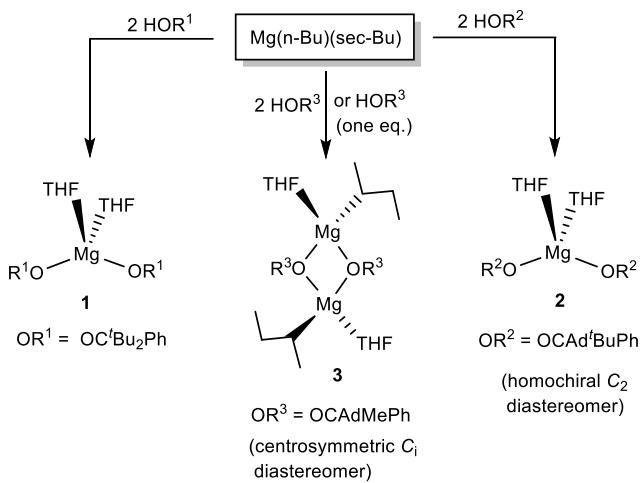


**Scheme 1.** Syntheses of the racemic alkoxide pro-ligands  $\text{HOAd}^{\text{R}}$  and  $\text{HOAdMePh}$ .

The pro-ligands were characterized by  $^1\text{H}$  and  $^{13}\text{C}$  NMR spectroscopy, IR and HRMS. The structure of  $\text{HOR}^2$  was also confirmed by the X-ray structure determination.  $\text{HOR}^2$  crystallized as a racemic mixture in the polar space group  $Pna2_1$ .

#### Coordination chemistry of $\text{HOR}^2$ and $\text{HOR}^3$ with magnesium

Coordination chemistry of  $\text{HOR}^2$  and  $\text{HOR}^3$  was explored by treating n-butyl-sec-butylmagnesium (0.7 M solution in hexane) with two equivalents of the racemic mixture of  $\text{HOR}^2$  and  $\text{HOR}^3$  (**Scheme 2**). Previously reported synthesis of  $\text{Mg}(\text{OR}^1)_2(\text{THF})_2$  (**1**) is also presented in **Scheme 2**. The reaction of  $\text{Mg}(\text{n-Bu})(\text{sec-Bu})$  with  $\text{HOR}^2$  led to the clean formation of  $\text{Mg}(\text{OR}^2)_2(\text{THF})_2$  (**2**), which was isolated as colorless crystals from  $\text{CH}_2\text{Cl}_2$  in 84% yield. **2** was characterized by NMR spectroscopy, X-ray crystallography, and elemental analysis. Elemental analysis confirms  $\text{Mg}(\text{OR}^2)_2(\text{THF})_2$  formulation. Most significantly,  $^1\text{H}$  NMR spectrum suggests the formation of a single diastereomer in solution.



**Scheme 2.** Reactivity of achiral alkoxides  $\text{HOR}^1$  and chiral (racemic) alkoxides  $\text{HOR}^2$  and  $\text{HOR}^3$  with n-butyl-sec-butylmagnesium.

As a general rule, the combination of a racemic alkoxide mixture can lead to the two different diastereomers in the resulting  $\text{Mg}(\text{OR}^2)_2(\text{THF})_2$  product: a homochiral isomer of an approximate  $C_2$  symmetry and a meso isomer of an approximate  $C_s$  symmetry. Due to their different physical properties, different diastereomers should give rise to different NMR spectra. However, the  $^1\text{H}$  NMR spectrum of **2** suggests the presence of a single species in solution, exhibiting one singlet for the  $^{\text{t}}\text{Bu}$  groups (1.38 ppm), two signals for the THF ligands (3.84 and 1.28 ppm) and five aromatic signals for the alkoxide phenyl group. Five different aromatic signals for the phenyl group are generally consistent with its restricted rotation, as previously described for  $\text{Mg}(\text{OR}^1)_2(\text{THF})_2$  (**1**,  $\text{OR}^1 = \text{OC}^{\text{t}}\text{Bu}_2\text{Ph}$ ). This pattern is consistent with the presence of a single diastereomer in solution. The presence of single species in solution indicates chiral resolution of the ligands to create a single diastereomer.

The solid state structure of **2** is consistent with the solution structure, demonstrating the formation of a single homochiral diastereomer of  $C_2$  symmetry (**Figure 1**). **2** crystallizes in the centrosymmetric group  $P-1$ ; both enantiomers (*RR* and *SS*) are found in the unit cell. The structure of the *RR* enantiomer is presented in **Figure 1** and selected bond distances and angles are provided in **Figure 1** caption.

Overall, the structure of **2** ( $\text{Mg}(\text{OR}^2)_2(\text{THF})_2$ ) is in line with all previous structures of  $\text{M}(\text{OR})_2(\text{THF})_2$  complexes,<sup>50-52</sup> including a closely related magnesium complex  $\text{Mg}(\text{OR}^1)_2(\text{THF})_2$  (**1**).<sup>40</sup> Similarly to **1**, complex **2** exhibits distorted tetrahedral geometry, with a narrow THF-Mg-THF angle of  $90.5(1)^\circ$ , and a broader RO-Mg-OR/RO-Mg-C angle of  $131.2(2)^\circ$ . The examination of the structure of **2** clearly indicates that it is approximately  $C_2$ -symmetric (see **Figure 1**) albeit the  $C_2$  symmetry is not crystallographic. The  $C_2$  symmetry of **2** implies the exclusive formation of the homochiral diastereomer. We postulate that the  $C_2$ -symmetric homochiral (*RR* and *SS*) diastereomer forms as a result of the steric gradient of the ligand, that pushes large adamantyl groups away from each other. One of the enantiomers (*RR*) is shown in **Figure 1**; the presence of the other enantiomer is implied by the centrosymmetric nature of the space group ( $P-1$ ).

In contrast to the reactivity of  $\text{HOR}^2$ , the reaction of  $\text{HOR}^3$  ( $\text{HOAdMePh}$ , two equivalents) with n-butyl-sec-butylmagnesium led to the formation of the product demonstrating broad NMR resonances. Recrystallization of the crude product produced colorless crystals of complex **3**. **3** is a dimeric complex of  $\text{Mg}_2(\text{OR}^3)_2(\text{sec-Bu})_2(\text{THF})_2$  composition (**Scheme 2**), that was characterized by X-ray crystallography, elemental analysis, and NMR.

Solid-state structure of **3** reveals incomplete substitution of the alkyl ligands in the  $\text{Mg}(\text{n-Bu})(\text{sec-Bu})$  precursor (**Figure 2**). The reaction of  $\text{Mg}(\text{n-Bu})(\text{sec-Bu})$  with one equivalent of  $\text{HOR}^3$  similarly formed complex **3**. We have previously shown that the protonolysis of the alkyl groups in  $\text{Mg}(\text{n-Bu})(\text{sec-Bu})$  with  $\text{HOR}^1$  takes place in two steps, with the more sterically accessible n-butyl being replaced first.<sup>32</sup>

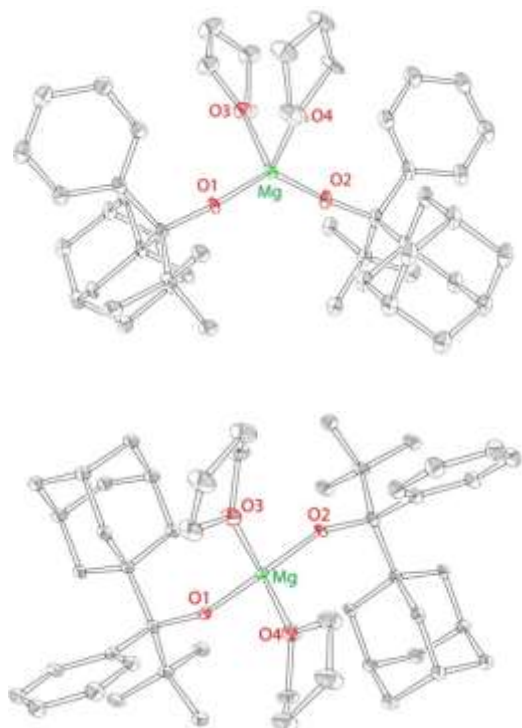


**Figure 1.** X-ray structure (50% probability ellipsoids) of the side view (left) and the top view (right) of **2**. H atoms and co-crystallized (disordered)  $\text{CH}_2\text{Cl}_2$  solvent are omitted for clarity. Only one enantiomer (*RR*) of the structure is shown. Another enantiomer (*SS*) can be generated by the inversion operation (*P-1*). Selected bond distances ( $\text{\AA}$ ) and angles ( $^\circ$ ) for **2**: Mg O1 1.842(4), Mg O2 1.831(4), O1 Mg O2 131.2(2), O3 Mg1 O4 90.5(1).

Similarly,  $\text{HOR}^3$  replaces *n*-butyl group first. However, the reaction of  $\text{Mg}(\text{n-Bu})(\text{sec-Bu})$  with one equivalent of  $\text{HOR}^1$  produced a mononuclear complex  $\text{Mg}(\text{OR}^1)(\text{sec-Bu})(\text{THF})_2$ , whereas **3** is dimer, in which the alkoxides are bridging, and *sec*-butyl and THF ligands are terminal. It is possible that it is due to the formation of the dimer only one of the alkyl groups undergoes facile substitution in the present case. We also note that the reaction of mononuclear  $\text{Mg}(\text{OR}^1)(\text{sec-Bu})(\text{THF})_2$  with one equivalent of  $\text{HOR}^1$  yielded complex **1**, whereas no reaction between dinuclear **3** and  $\text{HOR}^3$  is observed at room or elevated temperature (up to 80 °) in toluene (Figure S47).

Close examination of the structure of **3** suggests that the presence of the less sterically demanding methyl group (that points towards the *sec*-Bu and THF) is responsible for the dimeric structure. The reduced steric effect of the methyl-substituted  $[\text{OR}^3]$  pro-ligand enables a relatively sharp angle ( $85 \pm 1^\circ$ ) between the alkoxides at the same magnesium center. Finally, and in a sharp contrast to the  $C_2$ -symmetric symmetric structure of **2**, the symmetry of **3** is  $C_1$  (non-crystallographic), implying the presence of both *R* and *S* enantiomers in the same structure. Crystalline and analytically pure **3** still exhibits relatively broad and complicated  $^1\text{H}$  NMR spectrum, consistent with the presence of multiple species in solution.

It is possible that **3** undergoes monomer-dimer equilibrium in solution; such equilibrium could further lead to the formation of other species (such as the homochiral dimer, or the mixture

of  $\text{Mg}(\text{OR}^3)_2(\text{THF})_2$  and  $\text{Mg}(\text{sec-Bu})_2$ ). Collecting  $^1\text{H}$  NMR in toluene- $d_8$  at varying temperatures (25 ° – 80 °) has also produced broad and uninformative spectra (see Figure S26). We have also investigated the nature of complex **3** in solution by DOSY. The complex was prepared at concentrations of 5 and 10 mM, and DOSY experiments were performed on each. The resulting diffusion data were consistent between the samples (Figure S48). This suggests the complex is intact in the toluene solution, without a significant population of dissociated components. However, rapid dimer-monomer-dimer equilibrium in solution leading to the exchange of alkoxide/THF ligands can't be ruled out by this experiment; it is also likely to result in broad NMR spectrum. In light of the less well-defined structure of **3** (compared with **1** and **2**) in solution, its reactivity in polymerization was not investigated.

### Polymerization of *rac*-lactide

We have previously reported that complex **1** was a highly reactive catalyst for the ROP of racemic lactide (*rac*-LA), although the control degree over the polymerization process was modest. Herein, we explored the reactivity of complex **2**, that features bulkier and chiral alkoxides and compared its behavior with complex **1**. Representative ROP results are summarized in Table 1.

Initially, the reactivity of complex **2** was explored under the same reaction conditions used for complex **1** in our previous work: in  $\text{CH}_2\text{Cl}_2$  solution (10 mL), at 25 °, using 10  $\mu\text{mol}$  of the catalyst and varying lactide:catalyst ratios. The obtained results revealed a very high activity for catalyst **2** that was able to convert quantitatively up to 10000 equivalents of monomer within 15 minutes reaching the remarkable turnover frequency (TOF) of 39000  $\text{h}^{-1}$  (see run 9 of Table 1); a value fully comparable to the most active magnesium complexes reported in literature.<sup>47, 55-57</sup> The catalytic activity of complex **2** is significantly higher than that obtained for complex **1** (compare run 1 with 2 and run 4 with 5 of Table 1, respectively)<sup>40</sup> and for  $\text{Mg}(\text{BHT})_2\text{THF}_2$ ,<sup>58</sup> suggesting that the steric encumbrance around the magnesium center in  $[\text{Mg}(\text{OR})_2]$  precatalyst has an important role on the catalytic activity.

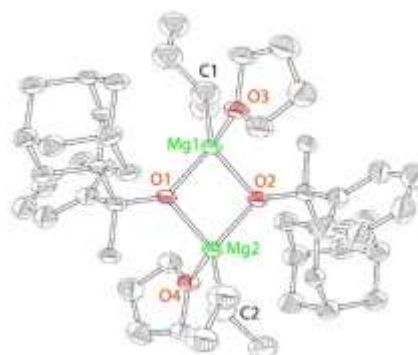


**Figure 2.** X-ray structure (50% probability ellipsoids) of **3**. H atoms are omitted for clarity. Only one enantiomer (*RR*) of the structure is shown. Selected bond distances ( $\text{\AA}$ ) and angles ( $^\circ$ ) for **3**: Mg1 O1 1.987(7), Mg1 O2 2.000(8), Mg1 O3 2.081(8), Mg1 C1 2.16(1), O1 Mg1 O2 84.4(3), O1 Mg2 O2 86.1(3), O3 Mg1 C1 128.0(5).

## ARTICLE

**Table 1.** Polymerizations of *rac*-LA promoted by **1** and **2**.<sup>a</sup>

<sup>a</sup> Run	Cat	<i>rac</i> -LA (eq)	B <sub>n</sub> OH (eq)	Time (min)	Solvent	<sup>b</sup> Conv. (%)	<sup>c</sup> <i>M</i> <sub>n</sub> (kDa)	<sup>c</sup> <i>D</i>
1	2	100	-	4	DCM	>99	3.0	3.30
2	1	100	-	60	DCM	56	4.7	2.26
3	2	200	-	4	DCM	>99	5.4	3.08
4	2	300	-	4	DCM	>99	7.6	2.04
5	1	300	-	60	DCM	43	4.1	2.56
6	2	600	-	10	DCM	>99	5.5	2.31
7	2	1000	-	15	DCM	>99	9.1	2.10
8	2	5000	-	15	DCM	>99	30.2	1.78
9	2	10000	-	15	DCM	97	72.6	1.83
10	2	100	-	30	Tol	>99	3.9	3.12
11	2	200	-	60	Tol	>99	6.5	2.62
12	2	300	-	60	Tol	>99	14.5	2.15
13	1	300	-	60	Tol	20	17.1	1.96
14	2	200	1	2	DCM	>99	18.6	1.79
15	2	200	1	0.5	DCM	70	8.1	1.59
16	2	200	1	0.5	THF	52	41.9	2.40
17	2	200	5	0.5	THF	87	5.3	1.23
18 <sup>d</sup>	2	10000	10	60	-	77	7.6	1.81
19 <sup>d</sup>	2	5000	50	60	-	48	3.6	1.56

<sup>a</sup> Reaction conditions: 10  $\mu$ mol of Mg, 10 mL of solvent, T= 25 °C (reaction times not optimized). <sup>b</sup>Determined by <sup>1</sup>H NMR. <sup>c</sup>Experimental *M*<sub>n</sub> and *D* values were determined by GPC analysis in THF using polystyrene standards corrected with the factor 0.58. <sup>d</sup> 10  $\mu$ mol of Mg T= 150 °C, technical grade L-LA.

It is possible that the presence of bulky alkoxides groups around magnesium disfavors aggregation phenomena that can occur in the polymerization medium, above all when an alcohol is used as cocatalyst, as observed by Miller<sup>58</sup> and Nifant'ev<sup>59</sup> that described the formation of dimeric species by reaction of the Mg(BHT)<sub>2</sub>THF<sub>2</sub> with benzyl alcohol.

As already observed for complex **1**, the activity decreased dramatically when the polymerizations were performed in toluene solution (runs 10-13, Table 1), while a little decrease was noted in the presence of a coordinating solvent as THF (see runs 16 and 17, Table 1). By adding one or more equivalents of benzyl alcohol as initiator, the performance of catalyst **2**

improved in both solvents, DCM (see runs 14 and 15, Table 1), and THF (see runs 16 and 17, Table 1).

Subsequently, catalyst **2** was tested under more challenging industrial-like conditions: bulk conditions, 150 °C, unpurified monomer (technical grade) and in the presence of a large excess of alcohol as chain transfer agent to improve the productivity of the catalyst (runs 18 and 19, Table 1). Also, in this case the catalyst preserved its high activity showing a TOF of 7700 h<sup>-1</sup>. All polymers produced were characterized by <sup>1</sup>H NMR, GPC and MALDI-ToF-MS analyses.

The microstructures of the resulting PLA samples were analyzed by <sup>1</sup>H NMR spectroscopy. For all samples, despite the chiral nature of complex **2**, the *P*<sub>m</sub> values were not higher than 0.56,

suggesting the lack of stereochemical control (Figure S27). However, no epimerization phenomenon was detected in the samples obtained with L-LA.

The molecular masses of PLA samples obtained in the absence of alcohol showed values significantly lower than those expected (although they increased with the number of equivalents of reacted monomer), and dispersities relatively high ( $1.59 < D < 3.30$ ). These features are indicative of a not well controlled process.

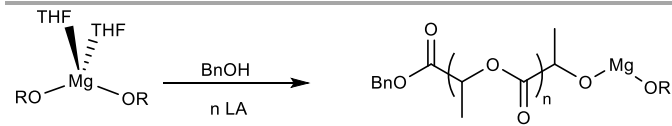
The MALDI-ToF spectra of the samples obtained in the exclusive presence of the magnesium complex **2** (run 1, Table 1) revealed a main distribution of peaks, with a spacing of  $72 \text{ g mol}^{-1}$ , corresponding to cyclic species derived by extensive intramolecular transesterification reactions (Figure S28).

A control over the properties of the resulting polymer can be improved significantly by the use of a coordinating solvent THF, and in the presence of 5 equivalents of alcohol as chain transfer agent (see run 17, Table 1). These polymerization conditions led to a relatively narrow dispersity ( $D = 1.23$ ). The molecular masses, evaluated by GPC and NMR, were consistent with the theoretical values calculated considering the amount of added alcohol. We postulate that the presence of five equivalents of alcohol as chain transfer agent enables fast and reversible exchange reactions between the active species and the dormant hydroxyl-ended chains. These are much more rapid than the chain initiation and propagation steps thereby ensuring that the rapid growing/dormant interconversion goes on over the entire polymerization process. Consequently, better control over the molecular masses is achieved. The MALDI-ToF spectrum (Figure S30) described linear chains with  $\text{BnO}$ - and -H end groups, while the presence of a major and minor series with a separation of 72 Da indicated that transesterification reactions may still occur.

For the sample obtained by technical grade lactide, predominant -OH chain end groups were observed, as consequence of a large presence of protic impurities into the monomer (Figure S31).

To shed light on the mechanism of polymerization and the nature of the active species involved, alcoholysis experiments were performed with both complexes (**2** and **1**) and one equivalent of alcohol ( $\text{BnOH}$  or  $\text{iPrOH}$ ) in  $\text{C}_6\text{D}_6$  or  $\text{CD}_2\text{Cl}_2$  solution. The  $^1\text{H}$  NMR spectra of the reaction mixtures showed the disappearance of added alcohols ( $\text{BnOH}$  or  $\text{iPrOH}$ ) and the production of  $\text{HOR}^1$  or  $\text{HOR}^2$  as free alcohols. At the same time, new metal species  $\text{Mg(OBn)(OR}^2)$  were observed, suggesting the substitution of one OR ligand with an OBn or O*Pr* group at the Mg center (Figures S32–S36). Analogous results were described for alcoholysis of  $\text{Mg(BHT)}_2(\text{THF})_2$ .<sup>59</sup>

After the addition of 10 equivalents of lactide, the monomer was rapidly consumed while the ligand remained in the polymerization medium as free ligand (Figures S36 and S37).



Scheme 3. Mechanisms of polymerization in the presence of alcohol.

Thus, when an exogenous alcohol was added in the polymerization medium, new asymmetric magnesium alkoxides were produced, and the monomer insertion occurred into the new Mg-alkoxide bond formed *in situ* while the free ligand was not able to act as chain transfer agent (Scheme 3).

#### Polymerization of lactones

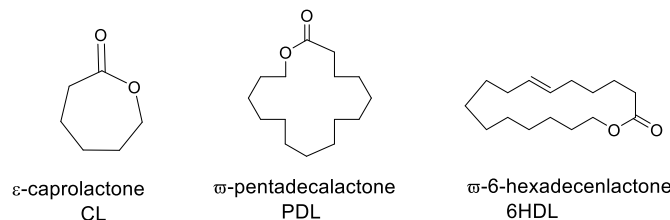
Based on the high activities obtained in the ROP of *rac*-lactide, we decided to extend the application of these systems to  $\epsilon$ -caprolactone ( $\epsilon$ -CL) and to less reactive substrates such as macrolactones, namely  $\omega$ -pentadecalactone (PDL) and  $\omega$ -6-hexadecenylactone (6-HDL) (Scheme 4). Their polymers can be imagined as the sustainable alternative to linear low-density polyethylene. Moreover, HDL is an unsaturated macrolide that offers the chance of simple post-polymerization functionalization.

The polymerization of lactones was generally performed in toluene solution in the presence of benzyl alcohol ( $\text{BnOH}$ ) as an initiator. Polymerization data are summarized in Table 2. Monomer conversions were evaluated during the polymerization using  $^1\text{H}$  NMR spectroscopy, by comparing the intensity of signal related to methylene protons adjacent to the ester group of the monomer, and the signal of the same protons within the polymer.

In the ROP of  $\epsilon$ -CL, the conversion of 160 equivalents of monomer was achieved after 0.5 min at room temperature (run 1, Table 2) showing a catalytic activity analogous to that achieved in the ROP of *rac*-LA and higher than that reported for  $\text{Mg(BHT)}_2(\text{THF})_2$ .<sup>60</sup> In this case, a good control over the molecular masses was observed, and the experimental values were coherent with those expected.

Both magnesium complexes revealed high activity in the polymerization of HDL, allowing the conversion of approximately 100 equivalents of monomer after 10 minutes (runs 2 and 4, Table 2) and showing the remarkable turnover frequencies (TOF) of 648 and 672  $\text{h}^{-1}$ , respectively. The quantitative conversion of HDL was achieved in 30 min (run 3, Table 2). Quite surprisingly, both complexes were able to promote the polymerization of HDL also at room temperature. These very mild reaction conditions are unusual for ROP of macrolactones (runs 7 and 8, Table 2).<sup>20</sup> As observed in other polymerizations, the activity of complex **2** was slightly higher than that of complex **1** (compare runs 5 and 6 and runs 7 and 8, Table 2).

The observed activities for complexes **1** and **2** were very high; similar magnesium complex  $\text{Mg(BHT)}_2(\text{THF})_2$  was able to convert only 50 equivalents of PDL after 5 hours under analogous reaction conditions.<sup>48</sup>



Scheme 4. Structures of lactones investigated in this work.

**Table 2.** Polymerization of macrolactones promoted by **1** and **2**.<sup>a</sup>

<sup>a</sup> Run	Cat	Lactone	T (eq)	Time (°C)	<sup>b</sup> Conv. (min)	TOF (%)	<sup>c</sup> M <sub>n</sub> (h <sup>-1</sup> )	<sup>c</sup> D (kDa)
1 <sup>e</sup>	1	ε-CL	25	0.5	76	18240	23.3	1.73
2	1	HDL	110	10	54	648	29.7	2.51
3	1	HDL	110	30	>99	400	66.0	3.19
4	2	HDL	110	10	56	672	31.0	2.26
5	1	PDL	110	10	48	600	26.4	2.13
6	2	PDL	110	10	74	920	37.2	2.18
7 <sup>d</sup>	1	HDL	25	1440	60	5	26.0	2.31
8 <sup>d</sup>	2	HDL	25	1440	>99	8	49.8	2.09

<sup>a</sup>Reaction conditions: 10  $\mu$ mol of Mg; 10  $\mu$ mol of benzyl alcohol; [monomer]/[catalyst]= 200:1, 0.5 mL of toluene; <sup>b</sup>Determined by  $^1$ H NMR. <sup>c</sup>Experimental  $M_n$  and  $D$  values were determined by GPC analysis in THF using polystyrene standards, while for PDL in  $\text{CHCl}_3$  using polystyrene standards. <sup>d</sup>solvent DCM 1mL, reaction time 24 h

The data suggest that the higher basicity of the OR ligands in comparison to phenoxy ligands could modulate more efficiently the Lewis acidity of the magnesium center with beneficial effects on the catalytic activity in the ROP of macrolactones. Figure 3 shows the  $^1\text{H}$  NMR spectrum of a typical poly(PDL) sample. In addition to the signals attributable to the methylene groups of the main chain, signals of low intensity are observed at 5.2 ppm and 3.5 ppm. These signals can be attributed to the methylene protons of benzylic  $-\text{OCH}_2\text{Ph}$  and alkyl  $\text{CH}_2\text{-CH}_2\text{-OH}$  end groups. In the  $^1\text{H}$  NMR spectrum of the poly(HDL), in addition to the same main resonances observed for the poly(PDL), a signal was evident at 5.4 ppm for the protons of the double bond of the repeating unit (Figure 4).

The GPC analysis of these polymers showed molecular masses consistent with the theoretically expected values and monomodal distributions (Figures S45 and S46). The dispersity values were around 2, as expected for macrolactone ROP and can be understood in terms of relatively similar rates of propagation and transesterification.

The end-group analysis of a low molecular weight sample of poly( $\omega$ -6-HDL) (prepared with a low monomer/Mg ratio of 20) using MALDI-TOF mass spectrometry similarly showed mostly distribution of OBn end-capped chains (Figure 5). In the range

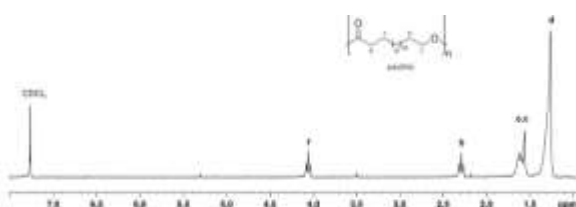


**Figure 3.**  $^1\text{H}$  NMR (300 MHz,  $\text{CDCl}_3$ , 298 K) spectrum of poly( $\omega$ -PDL).



**Figure 4.**  $^1\text{H}$  NMR (300 MHz,  $\text{CDCl}_3$ , 298 K) spectrum of poly(HDL).

of the analyzed masses (3000 - 8500 m/z), a second distribution was observed corresponding to cyclic structures (Figure S34). We note that in the ROP of macrolactones, linear chains are prevailingly produced. It is likely that the back-biting ring-closure reactions, responsible for the formation of cyclic polymers, are disfavored because of the long methylene sequences of the repeating units.<sup>48</sup>

## Copolymerization of maleic anhydride and propylene oxide

Poly(propylene fumarate) (PPF) is a biodegradable and biocompatible polymer which has been largely investigated for the preparation of biological scaffold since its unsaturated backbone can be used for photochemical cross-linking reactions in stereolithographic printing<sup>61, 62</sup> or suitable functionalizations.<sup>63, 64</sup> PPF was traditionally obtained by step-growth polycondensation, although this approach suffers from low yields, and lack of control over molecular masses.

In 2002, Hirabayashi and co-workers described a different strategy to obtain PPF by the ring-opening copolymerization of propylene oxide (PO) and maleic anhydride (MA) using magnesium diethoxide ( $[\text{Mg}(\text{OEt})_2]_n$ ) as the catalyst.<sup>65</sup> A

systematic exploration of several catalysts for MA/PO copolymerization was performed by Coates.<sup>66</sup> Recently, Becker and co-workers described the synthesis of poly(propylene fumarate) by the ring-opening copolymerization PO/MA with 2,6-di-tert-butylphenoxide magnesium in combination with a functionalized primary alcohol as initiator.<sup>27, 63</sup>

Considering the structural analogy between the magnesium catalyst used by Becker and the complexes described in this work, we decided to explore their behavior in the copolymerization of maleic anhydride with racemic propylene oxide (**Scheme 5**).

The polymerization reactions were initially performed at 80 °C and in the presence of a single equivalent of benzyl alcohol as initiator (**Table 3**).

A strong solvent effect on activity was observed for catalyst **1**; the best activity was achieved for reactions performed in bulk, while in hexane it decreased significantly (runs 1-3, **Table 3**). A higher selectivity was achieved in the absence of solvent while no difference was observed when a solvent was used. The molecular masses were similar to those obtained with related Mg catalysts.<sup>27</sup>

**Figure 5.** MALDI-TOF spectrum of poly(HDL) (reaction conditions see run 5 of Table 2, [HDL]/[Mg]=20).

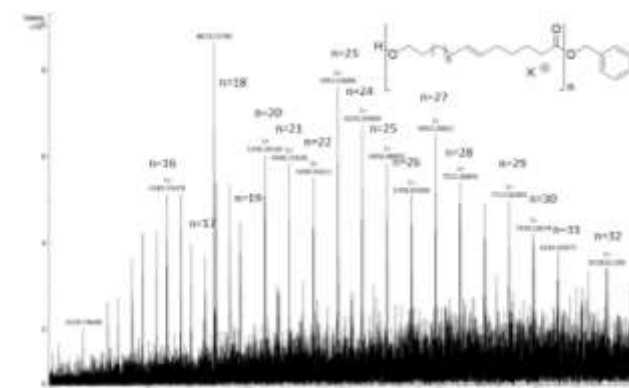


**Table 3.** Copolymerization of maleic anhydride and propylene oxide by **1** and **2**<sup>a</sup>

Run	Catalyst	Cocat	Solvent	T (°C)	time (h)	Conv <sup>b</sup> (%)	ester (%)	<sup>c</sup> M <sub>n</sub> (kDa)	<sup>c</sup> D
1	<b>1</b>	BnOH	Toluene	80	24	80	78	3.1	1.89
2	<b>1</b>	BnOH	Hexane	80	24	17	81	4.1	2.04
3	<b>1</b>	BnOH	-	80	24	>99	87	13.2	2.07
4	<b>1</b>	PPNCl	-	80	15	>99	>99	4.0	1.77
5	<b>1</b>	PPNCl	-	80	8	65	>99	1.1	2.02
6	<b>2</b>	PPNCl	-	80	8	54	>99	0.9	1.78
7	<b>2</b>	PPNCl	-	25	72	24	>99	2.2	1.99
8	-	PPNCl	-	25	72	<1	-	-	-

A significant increase in activity and selectivity was observed when the polymerization was performed in the presence of PPNCl (cfr runs 3 with 4 and 5, **Table 3**). A control experiment performed in the absence of catalyst (with PPNCl only) showed insignificant conversion of the monomers. A perfectly alternating structure was obtained, as evident by the absence of the resonances characteristic of polyether sequences at 3.5 ppm of the <sup>1</sup>H NMR spectrum (**Figure 6**) even when the copolymerization run to full conversion with an excess of PO (run 4, **Table 3**). As a result, further polymerization experiments were conducted by adding the onium salt (PPNCl) as cocatalyst. Both catalysts **1** and **2** showed the same reactivity and complete selectivity (runs 5 and 6, **Table 3**).

The regioregularity of the resultant PPMs was evaluated by the content of the head-to-tail (H-T) diads of PPM in the <sup>1</sup>H and <sup>13</sup>C NMR spectra (**Figures 7** and **8**). Both complexes were not regioselective. Consequently, atactic poly(propylene maleate)s were obtained in all cases as evident by the signals present at 130 ppm in the <sup>13</sup>C NMR spectrum (**Figure 8**).<sup>67</sup> No significant differences were observed when PPNCl was used as cocatalyst.



**Scheme 5.** Copolymerization of propylene oxide and maleic anhydride.

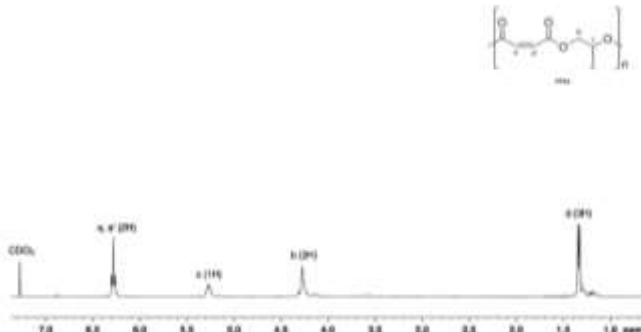


**Figure 6.** <sup>1</sup>H NMR (400 MHz, CDCl<sub>3</sub>, 298 K) spectrum of poly(propylene maleate)

## ARTICLE

<sup>a</sup>Reaction conditions: 10  $\mu$ mol of Mg complex; [MA]/[PO]/[Mg]/[Cocat] = 200/1500/1/1 solvent = 1 mL. <sup>b</sup>Conv. (%) is the conversion of MA, and ester (%) is the percentage of the ester linkage in the polymer. <sup>c</sup>Experimental  $M_n$  and  $D$  values were determined by GPC analysis in THF using polystyrene standards.

Subsequently, cis-trans isomerization of the C=C bonds in the polymer backbone of the poly(propylene maleate) was performed (**Scheme 6**). Quantitative isomerization of the cis-maleate groups to form the related trans-fumarates was carried out by the addition of a catalytic amount of diethylamine, as described in the literature.<sup>66</sup> A comparison of the proton spectra of PPM and PPF shown in **Figure 9** shows a shift in the alkene protons of the repeating unit, (from 6.28 to 6.86 ppm), while all other signals remain unchanged, confirming the isomerization of the chain. No change in either the molecular weight or the dispersity of the polymer was observed after the isomerization reaction.

Finally, complexes **1** and **2** were tested in the chemoselective terpolymerization of maleic anhydride (MA) and propylene oxide (PO) with lactide (LA), in order to obtain a di-block polyester (**Scheme 7**).

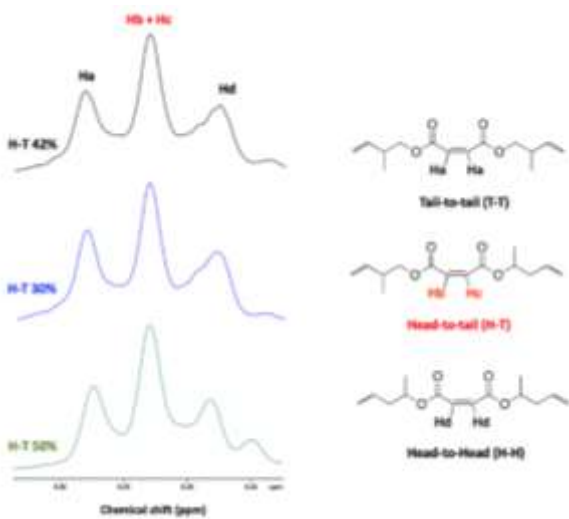
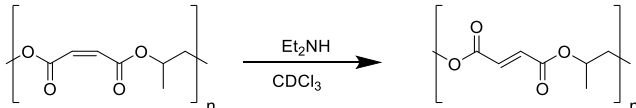


**Figure 7.** Analysis of the regiochemistry of PPMs using  $^1\text{H}$  NMR. Black curve: run 5, Blue curve: run 6. Green curve: run 1.



**Scheme 6.** Isomerization of poly(propylene maleate) to poly(propylene fumarate)



**Scheme 7.** Terpolymerization of maleic anhydride (MA), propylene oxide (PO) and rac-lactide (*rac*-LA).

The synthesis of poly(lactic acid) *block* poly(propylene fumarate) copolymers with well-defined composition was reported for the first time by Becker using copolymerization sequential procedures.<sup>68, 69</sup> Recently, block polyesters were obtained by chemoselective copolymerization from a multicomponent system formed by MA, PO, LA by bipyridine bisphenolate aluminum.

The polymerization tests were conducted at 80°C and in the absence of solvent. The reactions were carried out by mixing at the same time an excess of PO (1500 eq), 200 equivalents of MA, 100 equivalents of *rac*-LA, and 1 equivalent of PPNCl as co-catalyst. The polymerization was monitored by  $^1\text{H}$  NMR spectroscopy. After 16 hours, the anhydride conversion was quantitative for both catalysts while no conversion of the lactide was observed.

After 24 hours the *rac*-LA conversion was estimated to be around 50% for complex **1** and 62% for complex **2**.

The  $^1\text{H}$  NMR spectra (**Figure 8**) of the resulting polymers showed signals attributable to both blocks and were fully consistent with those previously reported.<sup>70</sup>

The DOSY spectrum (**Figure 9**) indicated that the resonances of the PLA sequences and of PPM portion showed the same diffusion coefficient, indicating that they belong to the same polymer chains. This finding supported the formation of di-

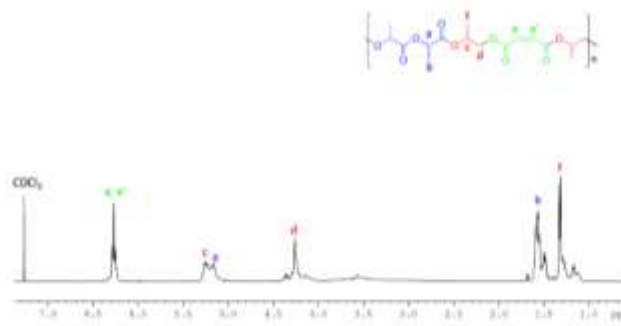
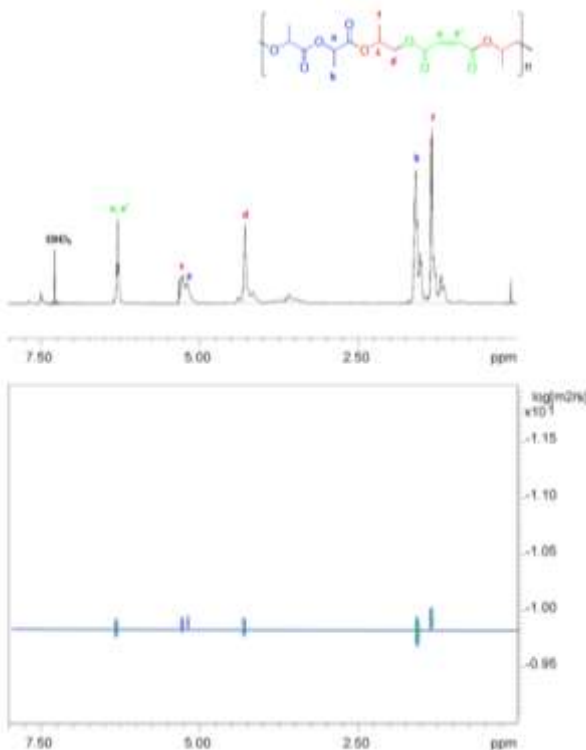


**Figure 8.**  $^1\text{H}$  NMR (400 MHz,  $\text{CDCl}_3$ , 298K) of the poly[(propylene maleate)-block-poly(lactic acid)] obtained by 1

**Figure 9.**  $^2$ D DOSY NMR (400 MHz,  $\text{CDCl}_3$ , 298 K) of the poly[(propylene maleate)-block-poly(lactic acid)]



block copolymer, namely poly(propylene maleate)-block-poly(lactic acid), by terpolymerization of PO, MA and *rac*-LA. Accordingly, the GPC analysis of the sample showed a monomodal distribution of the molecular masses with a  $M_n$  value of 3.5 KDa. This value agrees with the low molecular masses obtained in the ROCOP process that represents the first step of the whole terpolymerization, as already observed in other examples of switch catalysis ROCOP/ROP.<sup>28, 71-74</sup>

## Conclusions

In this work, we reported the synthesis of two new chiral bulky alkoxide ligands related to  $[\text{OC}^t\text{Bu}_2\text{Ph}]$ ,  $[\text{OC}^t\text{BuAdPh}]$  and  $[\text{OC}^t\text{BuMePh}]$  and studied the coordination chemistry upon reaction with *n*-butylsec-butylmagnesium. We demonstrated that while racemic  $[\text{OC}^t\text{BuAdPh}]$  enabled clean formation of homochiral  $C_2$ -symmetric complex  $\text{Mg}(\text{OC}^t\text{BuAdPh})_2(\text{THF})_2$ ,  $[\text{OC}^t\text{BuMePh}]$  did not exhibit well-defined coordination chemistry.

The reactivity of the new precatalyst  $\text{Mg}(\text{OCAd}^t\text{BuPh})_2(\text{THF})_2$  (**2**), along with the reactivity of the previously reported  $\text{Mg}(\text{OC}^t\text{Bu}_2\text{Ph})_2(\text{THF})_2$  (**1**), was investigated in the homopolymerization of lactide, lactones and copolymerization of maleic anhydride and propylene oxide. Likely due to the bulkier nature of the alkoxides, catalyst **2** revealed somewhat higher activity compared with catalyst **1** in the ROP of lactide.

When the polymerizations were performed in non-coordinating solvents, the molecular masses of PLAs were always significantly lower than theoretically expected values, because

of extensive intramolecular transesterification phenomena. In contrast, with the use of THF as solvent and benzyl alcohol as chain transfer agent, a better control of the molecular masses was obtained.

Both complexes showed high activity in the ROP of macrolactones such as  $\omega$ -pentadecalactone (PDL) and  $\omega$ -6-hexadecenolactone (6-HDL). In this case, linear polymeric chains with molecular masses consistent with the expected values were obtained.

Importantly, these catalysts were also active at room temperature. These reaction conditions are uncommon in the polymerization of these (relatively unreactive) monomers. This finding further contributes to the overall sustainability of our simple magnesium-alkoxide catalysts.

Finally, these complexes exhibited efficient copolymerization of maleic anhydride and propylene oxide, producing polypropylene fumarate with a perfectly alternating structure when the polymerization was performed in the absence of solvent or in the presence of PPNCl as cocatalyst. A fully biocompatible diblock polyester poly(propylene maleate)-block-polylactide was obtained combining the two synthetic routes in a one-pot procedure. In our future work, we will continue investigate homo- and copolymerization using these efficient, non-toxic, and cost-effective catalysts.

## Experimental Details

### Ligands and complexes: materials and methods

Reactions involving air-sensitive materials were performed under oxygen-free conditions in a Mbraun  $\text{N}_2$ -filled glovebox. *n*-Butyl-sec-butylmagnesium (0.7 M solution in hexane) was obtained from Sigma and used as received. All non-deuterated solvents (HPLC grade) were obtained from Sigma and dried using an MBraun solvent purification system. Deuterated solvents  $\text{C}_6\text{D}_6$  and  $\text{CDCl}_3$  were obtained from Cambridge Isotope Laboratories, and were dried over activated molecular sieves. All solvents were stored over 3 Å molecular sieves. Complexes were characterized by  $^1\text{H}$  and  $^{13}\text{C}$  NMR, X-ray crystallography, and elemental analysis. NMR spectra for metal complexes were recorded at the Lumigen Instrument Centre (Wayne State University) on an Agilent 400 and 600 MHz spectrometers in  $\text{C}_6\text{D}_6$  at room temperature. Chemical shifts and coupling constants ( $J$ ) were reported in parts per million ( $\delta$ ) and Hertz respectively. Elemental analysis was performed under ambient air-free conditions by Midwest Microlab LLC.  $\text{HOR}^1$  and  $\text{Mg}(\text{OR}^1)_2(\text{THF})_2$  (**1**) were prepared as previously described. The number-average molecular weights ( $M_n$ ) and molecular weight distributions of polymers (dispersity,  $D$ ) were evaluated by size exclusion chromatography (SEC), using Agilent 1260

Infinity Series GPC (ResiPore 3  $\mu$ m, 300  $\times$ 7.5 mm, 1.0 mL min $^{-1}$ , UV (250 nm) and refractive index (RI, PLGPC 220) detector. All measurements were performed with THF as the eluent at a flow rate of 1.0 mL/min at 35°C. Monodisperse poly(styrene) polymers were used as calibration standards

MALDI-ToF-MS analysis was performed on a Waters Maldi Micro MX equipped with a 337 nm nitrogen laser. The polymer sample was dissolved in THF with Milli-Q water containing 0.1% formic acid at a concentration of 0.8 mg mL $^{-1}$ . The matrix used was 2,5-dihydroxybenzoic acid (DHBA) (Pierce) and was dissolved in THF at a concentration of 30 mg mL $^{-1}$ .

#### Polymerization and polymer characterization: materials and methods

rac-Lactide was obtained from Sigma and purified by recrystallization from toluene, following by drying over  $P_2O_5$  for 72 h. Toluene and hexane (Sigma) were distilled under nitrogen over sodium. Cyclohexene oxide (CHO) and propylene oxide (PO) were purchased from Sigma-Aldrich and freshly distilled over  $CaH_2$ . Phthalic anhydride and maleic anhydride were purchased from Sigma and purified according to published procedure. Tetrahydrofuran (THF) was refluxed over Na and benzophenone and distilled under nitrogen. Monomers (Sigma-Aldrich) were purified before use:  $\omega$ -6-hexadecenolactone (6HDL),  $\omega$ -pentadecalactone, and cyclohexene oxide were distilled under vacuum on  $CaH_2$  and stored over 4  $\text{\AA}$  molecular sieves. Phthalic anhydride (PA) was crystallized from dry toluene.  $CDCl_3$  and toluene-d<sub>8</sub> were purchased from Eurisotop and used as received. Benzyl alcohol was purified by distillation over sodium. All other chemicals were commercially available and used as received. Mass spectra were acquired using a Bruker solariX XR Fourier transform ion cyclotron resonance mass spectrometer (Bruker Daltonik GmbH, Bremen, Germany) equipped with a 7 T refrigerated actively-shielded superconducting magnet (Bruker Biospin, Wissembourg, France). The polymer samples were ionized in positive ion mode using the MALDI ion source. The mass range was set to  $m/z$  200 – 5000. The laser power was 12% and 18 laser shots were used for each scan. Mass spectra were calibrated externally using a mix of peptide clusters in MALDI ionization positive ion mode. A linear calibration was applied. The polymer samples were dissolved in THF at a concentration of 1 mg/mL. The cationization agent used was potassium trifluoroacetate (Fluka, > 99 %) dissolved in THF at a concentration of 5 mg/mL. The matrix used was trans-2-[3-(4-tert-butylphenyl)-2-methyl-2-propenylidene]malononitrile (DCTB) (Fluka) and was dissolved in THF at a concentration of 40 mg/mL. Solutions of matrix, salt and polymer were mixed in a volume ratio of 4:1:4, respectively. The mixed solution was hand-spotted on a stainless steel MALDI target and left to dry. NMR spectra were recorded on Bruker Advance 400 spectrometer at 25 °C, unless otherwise stated. Chemical shifts ( $\delta$ ) are expressed as parts per million and coupling constants ( $J$ ) in hertz.  $^1H$  NMR spectra are referenced using the residual solvent peak at  $\delta$  = 7.27 for  $CDCl_3$ . Moisture and air-sensitive materials were manipulated under nitrogen using Schlenk techniques or an MBraun Labmaster glovebox.

#### X-ray crystallographic details

The structures of HOCA<sup>t</sup>BuPh (HOR<sup>2</sup>), Mg(OR<sup>2</sup>)<sub>2</sub>(THF)<sub>2</sub> (2), and Mg<sub>2</sub>(OR)<sub>3</sub>(THF)<sub>2</sub>(sec-Bu)<sub>2</sub> (3) were determined by X-ray crystallography. A Bruker Kappa APEX-II CCD diffractometer was used for data collection. A graphic monochromator was employed for the wavelength selection (MoK $\alpha$  radiation,  $\lambda$  = 0.71073  $\text{\AA}$ ). The data were processed using the APEX-2/3 software. The structures were solved and refined using SHELXT<sup>75</sup> and difference Fourier ( $\Delta F$ ) maps, as embedded in SHELXL-2018<sup>76</sup> running under Olex2<sup>77</sup>. The carbon hydrogen atoms were placed in calculated positions using a standard riding model and refined isotropically; all other atoms were refined anisotropically. The hydrogen on the oxygen in structure HOR<sup>2</sup> was located using the  $\Delta F$  maps. The structure of 2 contained co-crystallized disordered  $CH_2Cl_2$  molecule; the disorder was modeled by two alternate conformations. The crystal structure of 2 is a two-component non-merohedral twin (180° rotation around the [1 0 1] reciprocal rotation vector). Refinement was performed using the HKLF-5 file with reflections from both domains, which lead to a batch scale factor (BASF) parameter of 0.423(2). A solvent mask in Olex2 was applied for the structure Mg<sub>2</sub>(OR)<sub>3</sub>(THF)<sub>2</sub>(sec-Bu)<sub>2</sub> to remove a disordered ether (1.33 ethers/asymmetric unit) located along a solvent channel. A sec-Bu group was also disordered between two conformations.

Table 4. Experimental crystallographic parameters for HOR2, 2, and 3.

complex	HOR <sup>2</sup>	2	3
formula	$C_{21}H_{30}O$	$C_{50}H_{74}MgO_4 \times CH_2Cl_2$	$C_{52}H_{80}Mg_2O_4$
Fw, g/mol	298.45	848.32	914.34
temperature	100 K	100 K	100(2)K
cryst syst	orthorhombic	triclinic	monoclinic
space group	$Pna2_1$	$P-1$	$Pc$
color	colorless	Colorless	Colorless
$Z$	4	2	2
$a$ , $\text{\AA}$	9.3463(5)	12.352(6)	12.5905(10)
$b$ , $\text{\AA}$	13.8584(7)	13.519(6)	10.4610(9)
$c$ , $\text{\AA}$	12.5331(6)	15.032(7)	20.3664(17)
$\alpha$ , deg	90.00	67.339(13)	90
$\beta$ , deg	90.00	83.200(15)	90.778(2)
$\gamma$ , deg	90.00	82.150(14)	90
$V$ , $\text{\AA}^3$	1623.35(14)	2288.8(18)	2682.2(4)
$d_{calcd}$ , g/cm $^3$	1.221	1.231	1.132
$\mu$ , mm $^{-1}$	0.072	0.200	0.091
$2\theta$ , deg	52.74	51.112	51.016
$R_1^a$ (all data)	0.0728	0.1295	0.2148
$wR_2^b$ (all data)	0.0976	0.2400	0.3109
$R_1^a$ [( $I > 2\sigma$ )]	0.0604	0.0830	0.0959
$wR_2^b$ [( $I > 2\sigma$ )]	0.0933	0.2068	0.2430
GOF ( $F^2$ )	1.059	1.045	0.982

<sup>a</sup> $R_1 = \sum ||F_O - |F_C|| / \sum |F_O|$ . <sup>b</sup> $wR_2 = (\sum (w(F_O^2 - F_C^2)^2) / \sum (w(F_O^2)^2))^{1/2}$ . <sup>c</sup> GOF =  $(\sum w(F_O^2 - F_C^2)^2 / (n - p))^{1/2}$  where  $n$  is the number of data and  $p$  is the number of parameters refined.

**Synthesis of 1-Adamantyl *tert*-butyl Ketone.** This is a modification of the previously published procedure.<sup>78</sup> To a cold stirred pentane solution (3 mL) of 1-adamantanecarboxylic acid (0.50 g, 2.77 mmol), *tert*-butyllithium (1.7 M in pentane, 3.3 mL, 5.5 mmol) was added slowly (30 min). During the addition, the temperature was kept around -35 °C. After the addition was complete, the reaction was allowed to warm up to room temperature and stirred for additional 2 h, after which it was quenched by water. The organic phase was extracted by ether, dried over anhydrous MgSO<sub>4</sub>, filtered, and concentrated in vacuo to produce 1-adamantyl *tert*-butyl ketone as a white solid (71% yield). <sup>1</sup>H NMR (CDCl<sub>3</sub>, 600 MHz) δ 2.01 (m, 9H), 1.72 (bs, 6H), 1.24 (s, 9H); <sup>13</sup>C{<sup>1</sup>H} NMR (CDCl<sub>3</sub>, 150 MHz) δ 218.33, 48.92, 46.29, 39.72, 36.86, 28.58, 28.50; HR-MS m/z calcd for C<sub>15</sub>H<sub>25</sub>O [M+H]<sup>+</sup>: 221.1901, found: 221.1900, IR (cm<sup>-1</sup>): 2901 (s), 1674 (s), 1473 (w), 1134 (m), 995 (m).

**Synthesis of 1-Adamantyl Methyl Ketone.** To a cold stirred pentane solution (3 mL) of 1-adamantanecarboxylic acid (0.50 g; 2.77 mmol), MeLi (1.6 M in pentane, 3.5 mL, 5.5 mmol) was added slowly (30 min). During the addition, the temperature was kept at -35 °C. After the addition was complete, the reaction was allowed to warm up to room temperature and stirred for additional 2 h, after which it was quenched by water. The organic phase was extracted by ether, dried over anhydrous MgSO<sub>4</sub>, filtered, and concentrated in vacuo to produce 1-adamantyl methyl ketone as a white solid (62% yield). <sup>1</sup>H NMR (C<sub>6</sub>D<sub>6</sub>, 600 MHz) δ 1.80 (bs, 3H), 1.76 (s, 3H), 1.62 (d, J = 2.30, 6H), 1.54 (m, 3H), 1.48 (m, 3H); <sup>13</sup>C{<sup>1</sup>H} NMR (C<sub>6</sub>D<sub>6</sub>, 150 MHz) δ 211.41, 46.76, 38.81, 37.14, 28.71, 24.18 HR-MS m/z calcd for C<sub>12</sub>H<sub>19</sub>O [M+H]<sup>+</sup>: 179.1429, found: 179.1430.

**Synthesis of HOCAd<sup>t</sup>BuPh (HOR<sup>2</sup>).** To a cold ether solution of 1-adamantyl *tert*-butyl ketone (0.52 g, 2.4 mmol), phenyl lithium (1.9 M, 1.24 mL, 2.4 mmol) was added dropwise. The reaction was allowed to warm to room temperature and was stirred for 24 hours. After that, the volatiles were removed in vacuo and the product was extracted with hexane. The resulting solution was dried over anhydrous MgSO<sub>4</sub>, filtered, and concentrated in vacuo to give colorless crystals of HOR<sup>2</sup> (63% yield, 0.45 g, 1.5 mmol). <sup>1</sup>H NMR (C<sub>6</sub>D<sub>6</sub>, 600 MHz) δ 7.78 (d, J = 8.2 Hz, 1H), 7.46 (d, J = 7.0 Hz, 1H), 7.26 (m, 1H), 7.11 (m, 2H), 1.9 (d, J = 12 Hz, 3H), 1.84 (bs, 3H) 1.72 (d, J = 12 Hz, 3H), 1.63 (s, 1H), 1.54 (d, J = 12 Hz, 3H), 1.49 (d, J = 12 Hz, 3H), 1.05 (s, 9H); <sup>13</sup>C{<sup>1</sup>H} NMR (C<sub>6</sub>D<sub>6</sub>, 150 MHz) δ 145.54, 128.77, 126.59, 126.22, 83.65, 44.59, 42.57, 39.67, 37.61, 30.66, 29.90; HR-MS m/z calcd for C<sub>21</sub>H<sub>30</sub>O [M+H]<sup>+</sup>: 298.2243, found: 298.2305.

**Synthesis of HOCAdMePh (HOR<sup>3</sup>).** To a cold ether solution of 1-adamantyl methyl ketone (0.55 g, 3.1 mmol), phenyl lithium (1.9 M, 1.64 mL, 3.1 mmol) was added dropwise. The reaction was allowed to warm up to room temperature and was stirred for 24 h. After that, the volatiles were removed in vacuo and the crude product was extracted with hexane. The resulting solution was dried over anhydrous MgSO<sub>4</sub>, filtered, and concentrated in vacuo to give colorless crystals of HOR<sup>3</sup> (74% yield, 0.59 g, 2.3 mmol). Synthesis of HOCAdMePh has been recently reported.[ref] <sup>1</sup>H NMR (C<sub>6</sub>D<sub>6</sub>, 600 MHz) δ 7.38 (d, J = 7.6

Hz, 2H), 7.20 (t, J = 7.9 Hz, 2H), 7.11 (m, 1H), 1.87 (bs, 3H), 1.66 (m, 3H), 1.54 (m, 6H), 1.46 (m, 3H), 1.28 (s, 3H), 1.05 (s, 1H); <sup>13</sup>C{<sup>1</sup>H} NMR (C<sub>6</sub>D<sub>6</sub>, 150 MHz) δ 146.50, 128.14, 127.52, 126.83, 78.43, 39.74, 37.60, 37.10, 29.40, 24.33; HR-MS m/z calcd for C<sub>18</sub>H<sub>23</sub> [M-H<sub>2</sub>O+H]<sup>+</sup>: 239.1795, found: 239.1794, IR (cm<sup>-1</sup>): 3518 (br), 2893 (s), 1690 (w), 1489 (w), 1435 (w), 10856 (m), 709 (s).

**Synthesis of Mg(OR<sup>2</sup>)<sub>2</sub>(THF)<sub>2</sub> (2).** A 1 mL solution of HOR<sup>2</sup> (92 mg, 0.31 mmol) in ether was added dropwise to a 1 mL stirred solution of Mg(n-butyl)(sec-butyl) (21 mg, 0.15 mmol) in hexane. Following the addition, approximately 0.5 mL of THF was added, and the reaction mixture was allowed to stir for 2 h at room temperature. The subsequent work-up produced a white solid, which was recrystallized from concentrated CH<sub>2</sub>Cl<sub>2</sub> solution (-35 °C) to give Mg(OR<sup>2</sup>)<sub>2</sub>(THF)<sub>2</sub> in 84% yield (97 mg, 0.13 mmol). <sup>1</sup>H NMR (C<sub>6</sub>D<sub>6</sub>, 600 MHz) δ 8.09 (d, J<sub>HH</sub> = 7.9 Hz, 2H), 7.93 (d, J<sub>HH</sub> = 7.9 Hz, 2H), 7.36 (m, 2H), 7.27 (m, 2H), 7.22 (t, J<sub>HH</sub> = 6.9 Hz, 2H), 3.84 (m, 8H), 2.23 (m, 6H), 2.13 (d, J<sub>HH</sub> = 10.6 Hz, 6H), 2.07 (s, 6H), 1.75 (s, 12H) 1.38 (s, 18H) 1.27 (m, 8H). <sup>13</sup>C{<sup>1</sup>H} NMR (C<sub>6</sub>D<sub>6</sub>, 150 MHz) δ 153.27, 130.50, 129.69, 126.68, 125.58, 125.17, 84.71, 70.65, 45.73, 43.70, 40.86, 38.52, 32.39, 30.75, 25.32. Anal. calcd for: C<sub>50</sub>H<sub>74</sub>MgO<sub>4</sub> C, 78.72; H, 9.77 Found: C, 78.72 ; H, 9.94, IR (cm<sup>-1</sup>): 2963 (s), 2901 (m), 2832 (w), 1589 (w), 1474 (w), 1389 (w), 1358 (s), 1242 (m), 1204 (w), 1126 (m), 1096 (m), 1042 (m), 872 (s), 787 (m), 741 (m).

**Synthesis of Mg<sub>2</sub>(OR<sup>3</sup>)<sub>2</sub>(THF)<sub>2</sub>(sec-Bu)<sub>2</sub> (3). Reaction with 1:2 molar ratio:** A 1 mL solution of HOR<sup>3</sup> (60 mg, 0.234 mmol, 2.0 equiv) in diethyl ether and a 1 mL solution of Mg(n-butyl)(sec-butyl) (0.125 mmol, 1 equiv) in hexane were prepared. The solution of HOR<sup>3</sup> was then added dropwise to a stirring solution of Mg(n-butyl)(sec-butyl). Following the addition of the ligand, 0.5 mL of THF was added to the reaction mixture. The reaction mixture was stirred for 2 hours, upon which the volatiles were removed in vacuo. The resulting oily solid was extracted to diethyl ether, filtered and concentrated in vacuo to get white solid. Recrystallization from diethyl ether overnight produced **3** in 58% yield. The nature of **3** was confirmed by NMR (broad peaks), elemental analysis and X-ray crystallography. **Reaction with 1:1 molar ratio:** A 1 mL solution of HOR<sup>3</sup> (60 mg, 0.234 mmol, 1.0 equiv) in diethyl ether and a 1 mL solution of Mg(n-butyl)(sec-butyl) (0.238 mmol, 1.0 equiv) in hexane were prepared. The solution of HOR<sup>3</sup> was then added dropwise to a stirring solution of Mg(n-butyl)(sec-butyl). Following the addition of the ligand, 0.5 mL of THF was added to the reaction mixture. The reaction mixture was stirred for 2 hours, upon which the volatiles were removed in vacuo. The resulting oily solid was extracted to diethyl ether, filtered and concentrated in vacuo to get white solid. Recrystallization from diethyl ether overnight produced **3** in 46% yield. <sup>1</sup>H NMR (400 MHz, C<sub>7</sub>D<sub>8</sub>, room temperature) δ 7.70 (br s, 4H, OCAdMePh), 7.18 (br s, 4H, OCAdMePh), 7.08 (br s, 2H, OCAdMePh), 3.67 (s, 8H, THF), 2.02 (s, 6H, OCAdMePh), 1.19 (s, 8H, THF), 1.75-0.89 (Ad + sec-Bu resonances) ppm. <sup>1</sup>H NMR (400 MHz, C<sub>7</sub>D<sub>8</sub>, 80 °C) δ 7.55 (br s, 4H, OCAdMePh), 7.15 (br s, 4H, OCAdMePh), ~7.08 (br s, 2H, OCAdMePh), 3.67 (s, 8H, THF), 1.95 (s, 6H, OCAdMePh), 1.32 (s, 8H, THF), 1.69-0.86 (Ad + sec-Bu resonances) ppm. <sup>13</sup>C{<sup>1</sup>H} (C<sub>6</sub>D<sub>6</sub>, 100 MHz) δ 149.94, 128.92, 127.25, 127.05, 126.09, 80.12, 69.31, 40.27, 37.38, 34.10, 33.06,

29.58, 26.61, 25.14, 20.88, 17.33, 14.71 ppm. Anal. calcd for:  $C_{52}H_{80}Mg_2O_4$  C, 76.37; H, 9.86; Found: C, 76.69; H, 9.41.

**General procedure for the polymerization of lactide in solution.** Dichloromethane/toluene solution of 10  $\mu\text{mol}$  catalyst was mixed with a solution containing 100 equivalents (144 mg) of lactide in dichloromethane/toluene (total volume of the reaction was 10 mL,  $[\text{LA}] = 0.1 \text{ M}$ ). Reaction was stirred in room temperature for a given time after which it was stopped by adding 2-5 mL of methanol. PLA was precipitated in methanol and washed with excess methanol to remove all the impurities. For further purification, the polymer was dissolved using minimal amount of DCM and then added to 20 mL of methanol to precipitate pure PLA. Excess methanol was decanted, and the polymer was dried for 1 hour under vacuum. The reaction with 200, 300, 600, 1000, 5000, 10000, equivalents of lactide (0.2 M, 0.3 M, 0.6 M, 1M, 5M, and 10M respectively) in dichloromethane and 200, 300, 600, (0.2 M, 0.3 M, 0.6 M) toluene solutions was carried out in a similar fashion. The resulting polymer was characterized by  $^1\text{H}$  NMR spectroscopy, to determine degree of the polymerization. The methine region was also analyzed by homonuclear decoupled  $^1\text{H}$  NMR, to determine the tacticity of the polymer.

#### General procedure for the polymerization of lactide in bulk.

10  $\mu\text{mol}$  catalyst was mixed with 10000 equivalents (14.4 g) of lactide and 10 equivalent of benzyl alcohol in a pressure vessel. Reaction was heated at 150  $^{\circ}\text{C}$  for one hour.

#### General procedure for the co-polymerization of epoxides with cyclic anhydrides

**In bulk.** The copolymerization was performed in a Braun MBG20 glovebox. A magnetically stirred vial (10 mL) was charged with the anhydride. Subsequently, catalyst dissolved in neat epoxide was added, followed by co-catalyst. The vial was sealed with a Teflon lined cap and the reaction mixture was stirred at the desired temperature. At desired times, small aliquots of the reaction mixture were sampled, dissolved in  $\text{CDCl}_3$  and analyzed by  $^1\text{H}$  NMR spectroscopy. At the end of the polymerization, the product was dissolved in  $\text{CH}_2\text{Cl}_2$ , coagulated in diethyl ether and dried under vacuum oven. All analyses were performed on crude samples.

#### Acknowledgements

S. G. is grateful to the National Science Foundation (NSF) for current support under grant number CHE-1855681. Pro-ligands and Mg complexes were characterized at Lumigan Instrument Center.

M.M. thanks Dr Patrizia Iannece for Maldi ToF spectra, Dr Patrizia Oliva for NMR assistance, Dr Mariagrazia Napoli for GPC analysis.

**In solution.** The copolymerization was performed in an MBraun MBG20 glovebox at the desired temperature in 1mL of solvent. A magnetically stirred reactor vessel (10 mL) was charged with the anhydride. Subsequently, catalyst, co-catalyst and epoxide in 1 mL of solvent were added. The vial was sealed with a Teflon lined cap and the reaction mixture was stirred at 80  $^{\circ}\text{C}$ . At desired times, small aliquots of the reaction mixture were sampled, dissolved in  $\text{CDCl}_3$  and analyzed by  $^1\text{H}$  NMR spectroscopy. At the end of the polymerization, the product was dissolved in  $\text{CH}_2\text{Cl}_2$  and dried under vacuum oven. All analyses were performed on crude samples.

**Procedure for the terpolymerization of epoxides with cyclic anhydride and cyclic esters.** The terpolymerization was performed in a Braun MBG20 glovebox. A magnetically stirred vessel (10 mL) was charged with the anhydride and ester. Subsequently, catalyst dissolved in neat epoxide was added, followed by co-catalyst. The reaction mixture was stirred at the desired temperature. At desired times, small aliquots of the reaction mixture were sampled, dissolved in  $\text{CDCl}_3$  and analyzed by  $^1\text{H}$  NMR spectroscopy. At the end of the polymerization, the product was dissolved in  $\text{CH}_2\text{Cl}_2$ , coagulated in diethyl ether and dried under vacuum oven. All analyses were performed on crude samples.

#### Author Contributions

We strongly encourage authors to include author contributions and recommend using [CRediT](#) for standardised contribution descriptions. Please refer to our general [author guidelines](#) for more information about authorship.

#### Conflicts of interest

There are no conflicts to declare

#### Notes and references

1. L. Filiciotto and G. Rothenberg, *ChemSusChem*, 2021, **14**, 56-72.
2. P. B. V. Scholten, J. Cai and R. T. Mathers, *Macromolecular Rapid Communications*, 2021, **42**, 2000745.
3. I. van der Meulen, E. Gubbels, S. Huijser, R. Sablong, C. E. Koning, A. Heise and R. Duchateau, *Macromolecules* 2011, **44**, 4301-4305.
4. F. Stempfle, P. Ortmann and S. Mecking, *Chem. Rev.*, 2016, **116**, 4597-4641.
5. J. A. Wilson, Z. Ates, R. L. Pflughaupt, A. P. Dove and A. Heise, *Prog. Polym. Sci.*, 2019, **91**, 29-50.
6. L. Maisonneuve, T. Lebarb  , E. Grau and H. Cramail, *Polym. Chem.*, 2013, **4**, 5472-5517.

7. C. Liu, F. Liu, J. Cai, W. Xie, T. E. Long, S. R. Turner, A. Lyons and R. A. Gross, *Biomacromolecules*, 2011, **12**, 3291-3298.

8. M. Bouyahyi and R. Duchateau, *Macromolecules* 2014, **47**, 517-524.

9. T. Fuoco, A. Meduri, M. Lamberti, V. Venditto, C. Pellecchia and D. Pappalardo, *Polym. Chem.*, 2015, **6**, 1727-1740.

10. V. Ladelta, P. Bilalis, Y. Gnanou and N. Hadjichristidis, *Polym. Chem.*, 2017, **8**, 511-515.

11. V. Ladelta, J. D. Kim, P. Bilalis, Y. Gnanou and N. Hadjichristidis, *Macromolecules* 2018, **51**, 2428-2436.

12. T. Witt, M. Haeussler and S. Mecking, *Macromol. Rapid Commun.*, 2017, **38**, n/a.

13. A. E. Polloni, V. Chiaradia, E. M. Figura, J. P. De Paoli, D. de Oliveira, J. Vladimir de Oliveira, P. H. Hermes de Araujo and C. Sayer, *Appl. Biochem. Biotechnol.*, 2018, **184**, 659-672.

14. M. L. Focarete, M. Gazzano, M. Scandola, A. Kumar and R. A. Gross, *Macromolecules*, 2002, **35**, 8066-8071.

15. Z. Jiang, H. Azim, R. A. Gross, M. L. Focarete and M. Scandola, *Biomacromolecules*, 2007, **8**, 2262-2269.

16. S. Torron, M. K. G. Johansson, E. Malmstrom, L. Fogelstroem, K. Hult and M. Martinelle, 2017.

17. J. A. Wilson, S. A. Hopkins, P. M. Wright and A. P. Dove, *ACS Macro Lett.*, 2016, **5**, 346-350.

18. J. A. Nowalk, C. Fang, A. L. Short, R. M. Weiss, J. H. Swisher, P. Liu and T. Y. Meyer, *J. Am. Chem. Soc.*, 2019, **141**, 5741-5752.

19. M. P. F. Pepels, I. Hermsen, G. J. Noordzij and R. Duchateau, *Macromolecules* 2016, **49**, 796-806.

20. D. Myers, T. Witt, A. Cyriac, M. Bown, S. Mecking and C. K. Williams, *Polym. Chem.*, 2017, **8**, 5780-5785.

21. M. P. F. Pepels, M. Bouyahyi, A. Heise and R. Duchateau, *Macromolecules* 2013, **46**, 4324-4334.

22. I. van der Meulen, S. Huijser, E. Gubbels, C. E. Koning, A. Heise and R. Duchateau, *Polym. Prepr.*, 2011, **52**, No pp. given.

23. J. M. Longo, M. J. Sanford and G. W. Coates, *Chem. Rev.*, 2016, **116**, 15167.

24. Y. Zhu, C. Romain and C. K. Williams, *J. Am. Chem. Soc.*, 2015, **137**, 12179-12182.

25. R. A. Dilla, C. M. M. Motta, S. R. Snyder, J. A. Wilson, C. Wesdemiotis and M. L. Becker, *ACS Macro Lett.*, 2018, **7**, 1254-1260.

26. J. Guo, X. Liu, A. L. Miller, II, B. E. Waletzki, M. J. Yaszemski and L. Lu, *J. Biomed. Mater. Res., Part A*, 2017, **105**, 226-235.

27. J. A. Wilson, D. Luong, A. P. Kleinfeld, S. Sallam, C. Wesdemiotis and M. L. Becker, *J. Am. Chem. Soc.*, 2018, **140**, 277-284.

28. I. D'Auria, F. Santulli, F. Ciccone, A. Giannattasio, M. Mazzeo and D. Pappalardo, *ChemCatChem*, 2021, **13**, 3303-3311.

29. S. Kaler and M. D. Jones, *Dalton Trans.*, 2022, **51**, 1241-1256.

30. C. Gallegos, V. Tabernero, M. E. G. Mosquera, T. Cuenca and J. Cano, *Eur. J. Inorg. Chem.*, 2015, **2015**, 5124-5132.

31. C. Gallegos, V. Tabernero, F. M. Garcia-Valle, M. E. G. Mosquera, T. Cuenca and J. Cano, *Organometallics*, 2013, **32**, 6624-6627.

32. I. D'Auria, C. Tedesco, M. Mazzeo and C. Pellecchia, *Dalton Trans.*, 2017, **46**, 12217-12225.

33. S. D'Aniello, S. Laviéville, F. Santulli, M. Simon, M. Sellitto, C. Tedesco, C. M. Thomas and M. Mazzeo, *Catalysis Science & Technology*, 2022, DOI: 10.1039/D2CY01092E.

34. F. Santulli, M. Lamberti and M. Mazzeo, *ChemSusChem*, 2021, **14**, 5470-5475.

35. I. D'Auria, M. Lamberti, M. Mazzeo, S. Milione, G. Roviello and C. Pellecchia, *Chem. - Eur. J.*, 2012, **18**, 2349-2360.

36. T. Rosen, I. Goldberg, W. Navarra, V. Venditto and M. Kol, *Angew. Chem., Int. Ed.*, 2018, **57**, 7191-7195.

37. T. Rosen, Y. Popowski, I. Goldberg and M. Kol, *Chem. - Eur. J.*, 2016, **22**, 11533-11536.

38. T. Rosen, J. Rajpurohit, S. Lipstman, V. Venditto and M. Kol, *Chem. - Eur. J.*, 2020, **26**, 17183-17189.

39. I. E. Nifant'ev, A. V. Shlyakhtin, A. N. Tavtorkin, P. V. Ivchenko, R. S. Borisov and A. V. Churakov, *Catal. Commun.*, 2016, **87**, 106-111.

40. D. Wannipurage, T. S. Hollingsworth, F. Santulli, M. Cozzolino, M. Lamberti, S. Groysman and M. Mazzeo, *Dalton Trans.*, 2020, **49**, 2715-2723.

41. H. Xie, C. Wu, D. Cui and Y. Wang, *J. Organomet. Chem.*, 2018, **875**, 5-10.

42. R. Petrus and P. Sobota, *Coord. Chem. Rev.*, 2019, **396**, 72-88.

43. Y. Gao, Z. Dai, J. Zhang, X. Ma, N. Tang and J. Wu, *Inorg. Chem.*, 2014, **53**, 716-726.

44. C. W. Lee, S. Kuno and Y. Kimura, *Macromol. Res.*, 2013, **21**, 385-391.

45. R. Yang, G. Xu, C. Lv, B. Dong, L. Zhou and Q. Wang, *ACS Sustainable Chem. Eng.*, 2020, **8**, 18347-18353.

46. F. Santulli, M. Lamberti, A. Annunziata, R. C. Lastra and M. Mazzeo, *Catalysts*, 2022, **12**, 1193.

47. Y. Wang, W. Zhao, X. Liu, D. Cui and E. Y. X. Chen, *Macromolecules* 2012, **45**, 6957-6965.

48. J. A. Wilson, S. A. Hopkins, P. M. Wright and A. P. Dove, *Polym. Chem.*, 2014, **5**, 2691-2694.

49. I. E. Nifant'ev, A. V. Shlyakhtin, A. N. Tavtorkin, P. V. Ivchenko, R. S. Borisov and A. V. Churakov, *Catalysis Communications*, 2016, **87**, 106-111.

50. J. A. Bellow, D. Fang, N. Kovacevic, P. D. Martin, J. Shearer, G. A. Cisneros and S. Groysman, *Chem. Eur. J.*, 2013, **19**, 12225-12228.

51. J. A. Bellow, P. D. Martin, R. L. Lord and S. Groysman, *Inorg. Chem.*, 2013, **52**, 12335-12337.

52. J. A. Bellow, M. Yousif, D. Fang, E. G. Kratz, G. A. Cisneros and S. Groysman, *Inorg. Chem.*, 2015, **54**, 5624-5633.

53. J. S. Lomas and V. Bru-Capdeville, *J. Chem. Soc., Perkin Trans. 2*, 1994, DOI: 10.1039/P29940000459, 459-466.

54. A. Nagaki, H. Yamashita, Y. Tsuchihashi, K. Hirose, M. Takumi and J.-i. Yoshida, *Chem. Eur. J.*, 2019, **25**, 13719-13727.

55. Y. Sarazin, B. Liu, T. Roisnel, L. Maron and J.-F. Carpentier, *J. Am. Chem. Soc.*, 2011, **133**, 9069-9087.

56. M.-L. Shueh, Y.-S. Wang, B.-H. Huang, C.-Y. Kuo and C.-C. Lin, *Macromolecules*, 2004, **37**, 5155-5162.

57. V. Poirier, T. Roisnel, J.-F. Carpentier and Y. Sarazin, *Dalton Trans.*, 2011, **40**, 523-534.

58. H.-Y. Chen, L. Mialon, K. A. Abboud and S. A. Miller, *Organometallics*, 2012, **31**, 5252-5261.

59. I. E. Nifant'ev, A. V. Shlyakhtin, V. V. Bagrov, M. E. Minyaev, A. V. Churakov, S. G. Karchevsky, K. P. Birin and P. V. Ivchenko, *Dalton Trans.*, 2017, **46**, 12132-12146.

60. H.-J. Fang, P.-S. Lai, J.-Y. Chen, S. C. N. Hsu, W.-D. Peng, S.-W. Ou, Y.-C. Lai, Y.-J. Chen, H. Chung, Y. Chen, T.-C. Huang, B.-S. Wu and H.-Y. Chen, *Journal of Polymer Science Part A: Polymer Chemistry*, 2012, **50**, 2697-2704.

61. Y. Luo, C. K. Dolder, J. M. Walker, R. Mishra, D. Dean and M. L. Becker, *Biomacromolecules*, 2016, **17**, 690-697.

62. Y. Luo, G. Le Fer, D. Dean and M. L. Becker, *Biomacromolecules*, 2019, **20**, 1699-1708.

63. Y. Chen, J. A. Wilson, S. R. Petersen, D. Luong, S. Sallam, J. Mao, C. Wesdemiotis and M. L. Becker, *Angew. Chem., Int. Ed.*, 2018, **57**, 12759-12764.

64. Z. Cai, Y. Wan, M. L. Becker, Y.-Z. Long and D. Dean, *Biomaterials*, 2019, **208**, 45-71.

65. S. Takenouchi, A. Takasu, Y. Inai and T. Hirabayashi, *Polym. J. (Tokyo, Jpn.)*, 2002, **34**, 36-42.

66. A. M. DiCiccio and G. W. Coates, *J. Am. Chem. Soc.*, 2011, **133**, 10724-10727.

67. N. D. Harrold, Y. Li and M. H. Chisholm, *Macromolecules*, 2013, **46**, 692-698.

68. S. R. Petersen, J. A. Wilson and M. L. Becker, *Macromolecules* 2018, **51**, 6202-6208.

69. S. R. Petersen, J. Yu, T. R. Yeazel, G. Bass, A. Alamdari and M. L. Becker, *Biomacromolecules*, 2022, **23**, 2388-2395.

70. Y.-B. Wang, M.-Q. Wang, Y.-B. Shi, X.-L. Chen, D.-P. Song, Y.-S. Li and B. Wang, *Macromolecular Chemistry and Physics*, 2022, **223**, 2200079.

71. F. Isnard, M. Lamberti, C. Pellecchia and M. Mazzeo, *ChemCatChem*, 2017, **9**, 2972-2979.

72. F. Isnard, F. Santulli, M. Cozzolino, M. Lamberti, C. Pellecchia and M. Mazzeo, *Catal. Sci. Technol.*, 2019, **9**, 3090-3098.

73. F. Santulli, I. D'Auria, L. Boggioni, S. Losio, M. Proverbio, C. Costabile and M. Mazzeo, *Organometallics*, 2020, **39**, 1213-1220.

74. I. D'Auria, S. D'Aniello, G. Viscusi, E. Lamberti, G. Gorras, M. Mazzeo and D. Pappalardo, *Polymers*, 2022, **14**.

75. G. Sheldrick, *Acta Crystallographica Section A*, 2015, **71**, 3-8.

76. G. Sheldrick, *Acta Crystallographica Section C*, 2015, **71**, 3-8.

77. O. V. Dolomanov, L. J. Bourhis, R. J. Gildea, J. A. K. Howard and H. Puschmann, *Journal of Applied Crystallography*, 2009, **42**, 339-341.

78. G. A. Olah, A. H. Wu and O. Farooq, *J. Org. Chem.*, 1989, **54**, 1375-1378.